Pair Creation of Scalar Particles in Intense Bichromatic Laser Fields

Martin J A Jansen and Carsten Müller
Institut für Theoretische Physik I, Heinrich-Heine-Universität, 40225 Düsseldorf, Germany
E-mail: martin.jansen@tp1.uni-duesseldorf.de

Abstract. The creation of scalar particle pairs due to the decay of a highly energetic gamma quantum traveling in a laser field comprising two independent modes is considered. Employing the framework of strong-field scalar QED, detailed calculations aiming at two different aspects of the process are presented. We first investigate interference effects between reaction channels with absorption of different numbers of laser photons with commensurate frequency and demonstrate the possibility of coherent phase control. Then we study numerically a scheme of dynamical assistance, which offers prospects for an experimental realization of a Schwinger-like pair production process.

1. Introduction

The collision of two energetic photons can lead to the creation of electron-positron pairs and is known as the Breit-Wheeler process [1]. Employing instead a laser of frequency ω, a certain number n of laser photons may contribute to the pair creation process [2, 3, 4], which can be written symbolically as

$$\omega_\gamma + n\omega \to e^+e^-, \tag{1}$$

where ω_γ is the frequency of the gamma quantum. This multiphoton Breit-Wheeler process has already been verified experimentally in the SLAC-E144 experiment [5].

Proceeding to a high laser field-strength E while keeping its photon energy small, such that the field-strength parameter $\xi = eE/m\omega$ clearly exceeds unity while $\chi = 2\xi\,\omega_\gamma\omega/m^2 \ll 1$, the particle creation rate scales as [2, 3]

$$\mathcal{R} \sim \frac{\alpha m^2}{\omega_\gamma}\chi^{3/2}\exp\left(-\frac{8}{3\chi}\right) \tag{2}$$

revealing a non-analytic dependence on the laser field-strength. Here, α denotes the fine-structure constant, m the electron mass, and we use relativistic units with $\hbar = c = 1$. A similar behavior is seen for the famous Schwinger effect [6, 7], which refers to the creation of electron-positron pairs from the vacuum resulting from the application of a constant electric field. This fundamental effect has not yet been seen experimentally due to the high field strength $E \sim E_{\rm cr} = m^2/e \approx 10^{16}\,\mathrm{V/cm}$ required.

In this contribution, we will investigate a setup comprising two co-propagating laser beams of different frequencies and intensities which both give contributions to the pair creation process

induced by the collision with an additional counter-propagating gamma quantum. Symbolically, we have

$$\omega_\gamma + n_1\omega_1 + n_2\omega_2 \to e^+e^-, \tag{3}$$

where the indices $1, 2$ refer to the respective laser mode. The addition of the second reaction channel facilitates quantum mechanical interferences [8], which are most prominent for low-intensity lasers and may affect the angular distribution of the particles as well as the total rate; see [9, 10, 11] for related studies on the Bethe-Heitler process. We will demonstrate these effects by investigating the influence of a relative phase shift between the laser modes.

Furthermore, following the proposal of dynamical assistance [12], we demonstrate how a suitable combination of a high-intensity yet low-frequency laser with an additional low-intensity yet high-frequency laser can drastically increase the Schwinger-like pair creation process and finally render the effect visible in today's labs.

We will present detailed calculations following an S matrix approach within strong-field scalar QED, allowing us to treat the laser field non-perturbatively. For the sake of analytical simplicity, we neglect the particle spin. Nevertheless, we shall denote the produced particles as electrons and positrons. For an investigation of spin effects in intense fields, we refer to [13, 14]. Recent studies on Breit-Wheeler pair production in intense laser pulses can be found in [15, 16, 17].

2. Theoretical Framework

The pair creation process is formally described as the transition of a laser-dressed (spinless) electron from the negative to the positive continuum induced by the absorption of the gamma quantum, which is described as a single mode of the quantized radiation field. The depleted particle state with negative energy finally corresponds to the anti-particle.

The transition amplitude is given by the S matrix element

$$S = -i \int dt \, \langle \Psi_{p_-} | \hat{H}_{\text{int}} | \Psi_{p_+,\gamma} \rangle \tag{4}$$

where the initial state $|\Psi_{p_+,\gamma}\rangle = \Phi_{p_+}|\mathbf{k}_\gamma \lambda_\gamma\rangle$ is a product state of the laser-dressed electron with negative energy given by the state Φ_{p_+} and a singly occupied radiation mode with wave four vector $k^\mu_\gamma = (\omega_\gamma, \mathbf{k}_\gamma)$ and mode index λ_γ. The final state $|\Psi_{p_-}\rangle = \Phi_{p_-}|0\rangle$ contains the laser-dressed electron in the positive continuum and the depopulated radiation mode. The absorption of the gamma quantum is described by the field operator

$$\hat{\mathbf{A}}_\gamma = \sqrt{\frac{2\pi}{V\omega_\gamma}} \, \mathrm{e}^{-i(k_\gamma x)} \, \boldsymbol{\epsilon}_\gamma \, \hat{c}_{\mathbf{k}_\gamma \lambda_\gamma} \tag{5}$$

with polarization vector $\boldsymbol{\epsilon}_\gamma$, annihilation operator $\hat{c}_{\mathbf{k}_\gamma\lambda_\gamma}$ and a normalizing volume V. The interaction Hamiltonian thus reads

$$\hat{H}_{\text{int}} = -ie \left(\hat{\mathbf{A}}_\gamma \cdot \overrightarrow{\boldsymbol{\nabla}} - \overleftarrow{\boldsymbol{\nabla}} \cdot \hat{\mathbf{A}}_\gamma \right) + 2e^2 \mathbf{A}_L \cdot \hat{\mathbf{A}}_\gamma \tag{6}$$

where $\mathbf{A}_L$ is the vector potential of the laser field.

The laser field consists of two independent modes of frequencies ω_j, $j = 1, 2$ which are linearly polarized in orthogonal directions $\mathbf{e}_j$ and propagate in the same direction $\mathbf{n}$. Its vector potential in radiation gauge accordingly reads

$$\mathbf{A}_L = \mathbf{A}_1 + \mathbf{A}_2 \ , \ \mathbf{A}_j(\eta_j) = a_j \cos(\eta_j - \varphi_j) \, \mathbf{e}_j \tag{7}$$

where we have introduced phase variables $\eta_j = (k_j x) = \omega_j(t - \mathbf{n}\cdot\mathbf{r})$, which are related to the wave four vectors $k_j^\mu = \omega_j(1,\mathbf{n})$, and phase shifts φ_j. We measure the amplitudes in a Lorentz-invariant manner with $\xi_j = \frac{ea_j}{m}$.

We obtain the laser-dressed states for a particle with charge $\pm e$ and free four-momentum $p_\pm^\mu = (E_{p_\pm}, \mathbf{p}_\pm)$ from the Gordon-Volkov states

$$\Phi_{p_\pm}(x) = \frac{1}{\sqrt{2E_{p_\pm}V}}\,\mathrm{e}^{i[\pm(p_\pm x)-\Lambda_1-\Lambda_2]} \tag{8}$$

which, due to the perpendicular polarization directions, separate into contributions from each laser mode alone with

$$\Lambda_j = \frac{1}{(k_j p_\pm)}\int^{\eta_j}[e\mathbf{p}_\pm\cdot\mathbf{A}_j(\tilde\eta) \mp e^2\mathbf{A}_j^2(\tilde\eta)]d\tilde\eta\,. \tag{9}$$

The interaction between the particles and the laser-field is hereby taken into account non-perturbatively.

The time-averaged motion of the particles in the laser field is reflected in the laser-dressed momenta $q_\pm^\mu = p_\pm^\mu + 2k_1^\mu y_1^\pm + 2k_2^\mu y_2^\pm$, which occur naturally in this approach and are expressed using the abbreviation $y_j^\pm = \frac{e^2a_j^2}{8(k_j p_\pm)}$. The particles experience a mass increase by virtue of $(q_\pm q_\pm) = m_*^2$, leading to the laser-dressed mass $m_* = m[1+\frac{1}{2}(\xi_1^2+\xi_2^2)]^{1/2}$.

In order to carry out the space-time integration in Eq. (4), the integrand can be Fourier decomposed using generalized Bessel functions $\tilde J_n(u,v)$ which fulfill $\mathrm{e}^{i(u\sin(\phi)+v\sin(2\phi))} = \sum_{n=-\infty}^{\infty}\tilde J_n(u,v)\mathrm{e}^{in\phi}$. The generalized Bessel functions can be written in terms of ordinary Bessel functions as $\tilde J_n(u,v) = \sum_{l=-\infty}^{\infty} J_{n-2l}(u)J_l(v)$ [18]. Applying this method to each of the laser modes separately, we finally arrive at

$$S = S_0\sum_{n_1,n_2=-\infty}^{\infty} M_{n_1,n_2}\,\mathrm{e}^{i(n_1\varphi_1+n_2\varphi_2)}\mathrm{e}^{i(h_1+h_2)}(2\pi)^4\delta^4\left(q_- + q_+ - k_\gamma - n_1k_1 - n_2k_2\right) \tag{10}$$

with the prefactor $S_0 = -iem\sqrt{\pi/(2V^3E_{p_+}E_{p_-}\omega_\gamma)}$ and abbreviations $h_j = h_j^+ + h_j^-$, $h_j^\pm = x_j^\pm\sin(\varphi_j) + y_j^\pm\sin(2\varphi_j)$ and $x_j^\pm = \mp\frac{ea_j\mathbf{p}_\pm\cdot\mathbf{e}_j}{(k_jp_\pm)}$ for $j = 1,2$. We introduce the reduced matrix element

$$\begin{aligned} M_{n_1,n_2} \;=\; & \frac{(\mathbf{p}_- - \mathbf{p}_+)\cdot\boldsymbol{\epsilon}_\gamma}{m}\tilde J_{n_1}\tilde J_{n_2} \\ & + \xi_1(\mathbf{e}_1\cdot\boldsymbol{\epsilon}_\gamma)\left(\tilde J_{n_1+1} + \tilde J_{n_1-1}\right)\tilde J_{n_2} \\ & + \xi_2(\mathbf{e}_2\cdot\boldsymbol{\epsilon}_\gamma)\left(\tilde J_{n_2+1} + \tilde J_{n_2-1}\right)\tilde J_{n_1} \end{aligned} \tag{11}$$

where the arguments of the generalized Bessel functions $\tilde J_{n_j}$ and $\tilde J_{n_j\pm1}$ are $u_j = -(x_j^+ + x_j^-)$ and $v_j = -(y_j^+ + y_j^-)$. The δ-function in Eq. (10)

$$d_n = (2\pi)^4\delta^4\left(q_- + q_+ - k_\gamma - n_1k_1 - n_2k_2\right) \tag{12}$$

provides energy-momentum conservation for the process and motivates us to interpret the indices n_j as numbers of photons being absorbed in order to create the pair. Note that the conservation conditions include the dressing of the particles. From now on we abbreviate $n = (n_1, n_2)$.

The total particle creation rate $\mathcal{R}$ is obtained by integrating the amplitude squared over all possible particle states, averaging over the polarization states of the gamma quantum and finally dividing by the interaction time T, leading to

$$\mathcal{R} = \frac{1}{2}\sum_{\lambda_\gamma}\int\frac{Vd^3p_+}{(2\pi)^3}\int\frac{Vd^3p_-}{(2\pi)^3}\frac{|S|^2}{T}\ . \tag{13}$$

In order to obtain the square of the amplitude, we introduce primed indices n_1', n_2' and note that the product $d_n d_{n'}$ only allows contributions if

$$(n_1 - n_1')\omega_1 = (n_2' - n_2)\omega_2 \tag{14}$$

such that we are left with

$$|S|^2 = |S_0|^2 TV \sum_{\substack{n_1,n_2,n_1',n_2':\\(14)}} M_n M_{n'}^* d_n \mathrm{e}^{i[(n_1-n_1')\varphi_1+(n_2-n_2')\varphi_2]} \tag{15}$$

where the factors TV stem from the square of the δ-functions.

We see that for incommensurate frequencies, condition (14) can never be fulfilled, such that no interference terms appear and only ordinary terms with $n_j = n_j'$ contribute. On the other hand, for frequencies that are in a commensurate ratio, interference terms can be expected. Their contribution to the total process is modulated by the phase factor $\mathrm{e}^{i[(n_1-n_1')\varphi_1+(n_2-n_2')\varphi_2]}$. The sum over all possible photon number combinations includes the term (n_1, n_2, n_1', n_2') as well as the related term (n_1', n_2', n_1, n_2), where n_j and n_j' have been interchanged. Since the product of the reduced matrix elements is insensitive to this exchange, it is sufficient to regard in the following the sum of these two terms, which is modulated by $2\cos[(n_1 - n_1')\varphi_1 + (n_2 - n_2')\varphi_2]$. The distinction between primed and unprimed photon numbers is a purely mathematical effect, which cannot be seen in the experiment. Additionally we remark that for a term with $n_j \neq n_j'$, the numbers n_j are lacking a straightforward interpretation.

3. Interference Effects

In this section, we investigate interference effects which occur in a setup of two co-propagating lasers with a frequency ratio of 2. The intensities are chosen small ($\xi_j \ll 1$), such that the process can be regarded perturbatively. This means, by Taylor expanding the generalized Bessel function, we see that the term with photon numbers (n_1', n_2', n_1, n_2) scales as

$$\mathcal{R}_{(n_1',n_2',n_1,n_2)} \sim \xi_1^{|n_1|+|n_1'|}\xi_2^{|n_2|+|n_2'|}\ . \tag{16}$$

Therefore only terms featuring the smallest possible non-negative photon numbers and fulfilling the condition (14) contribute significantly. Additionally, we choose the intensities of the two modes such that the total particle count rates obtained for each mode alone are of the same order. This way, we keep the two modes in balance in order to maximize the visibility of interference effects.

Due to the small intensities applied here, the dressing of the particles may be neglected. Assuming the second mode to have the larger frequency, we fix the ratio of the frequencies $\nu = \omega_2/\omega_1$. Calculating the total particle count rate for each mode alone, we see that the condition of balanced contributions leads to

$$\xi_2 \sim \xi_1^\nu\ , \tag{17}$$

such that Eq. (16) reads

$$\mathcal{R}_{(n_1',n_2',n_1,n_2)} \sim \xi_1^{2N} \tag{18}$$

for non-negative photon numbers. We have introduced the number $N = n_1 + \nu n_2$ and we see that $n_1' + \nu n_2' = N$ in accordance with condition (14).

We carry out the calculations in the center of mass system, which implies

$$n_1\omega_1 + n_2\omega_2 = N\omega_1 = \omega_\gamma \tag{19}$$

and

$$n_1\omega_1 + n_2\omega_2 + \omega_\gamma = 2N\omega_1 = E_{p_+} + E_{p_-} \tag{20}$$

We see that processes with constant ν and N are of the same order and share a common center of mass system. The number N is related to the minimal photon numbers required: We would need either $n_1^{min} = N$ photons from the first or $n_2^{min} = N/\nu$ photons from the second mode in order to create the pair if the lasers were operated separately.

In order to measure the frequencies, we use the relativistic β parameter of the particles in their c.m. frame, and from Eq. (20) we obtain

$$\gamma = \frac{1}{\sqrt{1-\beta^2}} = \frac{N\omega_1}{m} \tag{21}$$

In the following, we investigate the angular distributions of the positrons, i.e. $\frac{d\mathcal{R}}{d\theta d\phi}$, with usual spherical coordinates θ and ϕ which describe the emission direction of the positron. Since we are working in the center of mass system, the electron is emitted in the opposite direction. The polar angle θ is measured with respect to the propagation direction of the lasers, while the azimuthal angle ϕ is measured in the polarization plane with $\phi = 0$ $(\pi/2)$ being the polarization axis of the first (second) mode. We carry out our calculations analytically and present our results without a common prefactor $\frac{\alpha m}{16\pi}\xi_1^{2N}$. The amplitude of the second laser is always chosen as $\xi_2 = 0.78\xi_1^2$, ensuring balanced contributions for both of the following cases.

3.1. Case I

In the first case, we choose the frequencies of our lasers such that either two photons from the first or one photon from the second mode are sufficient to create the pair, such that $\nu = 2 = N$. In addition to the ordinary processes with photon numbers $(2, 2; 0, 0)$ and $(0, 0; 1, 1)$, we have an interference term with $(2, 0; 0, 1)$. Figure 1 shows the angular distributions for different values of the frequencies (left to right) and for different values of the phase shift δ_1 (top to bottom), while $\delta_2 = 0$. The vertical axis shows the angle θ, while ϕ is depicted on the horizontal axis. The frequencies of the lasers are subject to upper limits at which even less photons would be sufficient to create the pair. For a fixed number N, this threshold is related to a maximum beta parameter

$$\beta_N = \frac{1}{\sqrt{N}}\,. \tag{22}$$

As the figures reveal, the emission happens mostly in the plane of polarization. The distribution is generally asymmetric about ϕ, but for certain values of the phase shift $\delta_1 = \pi/4$, it becomes symmetric. The asymmetry is caused by the interference contribution, which vanishes identically at this point. We see that the angular distribution strongly depends on the frequencies of the lasers; for higher frequencies, the regions of highest emission probability become more pronounced.

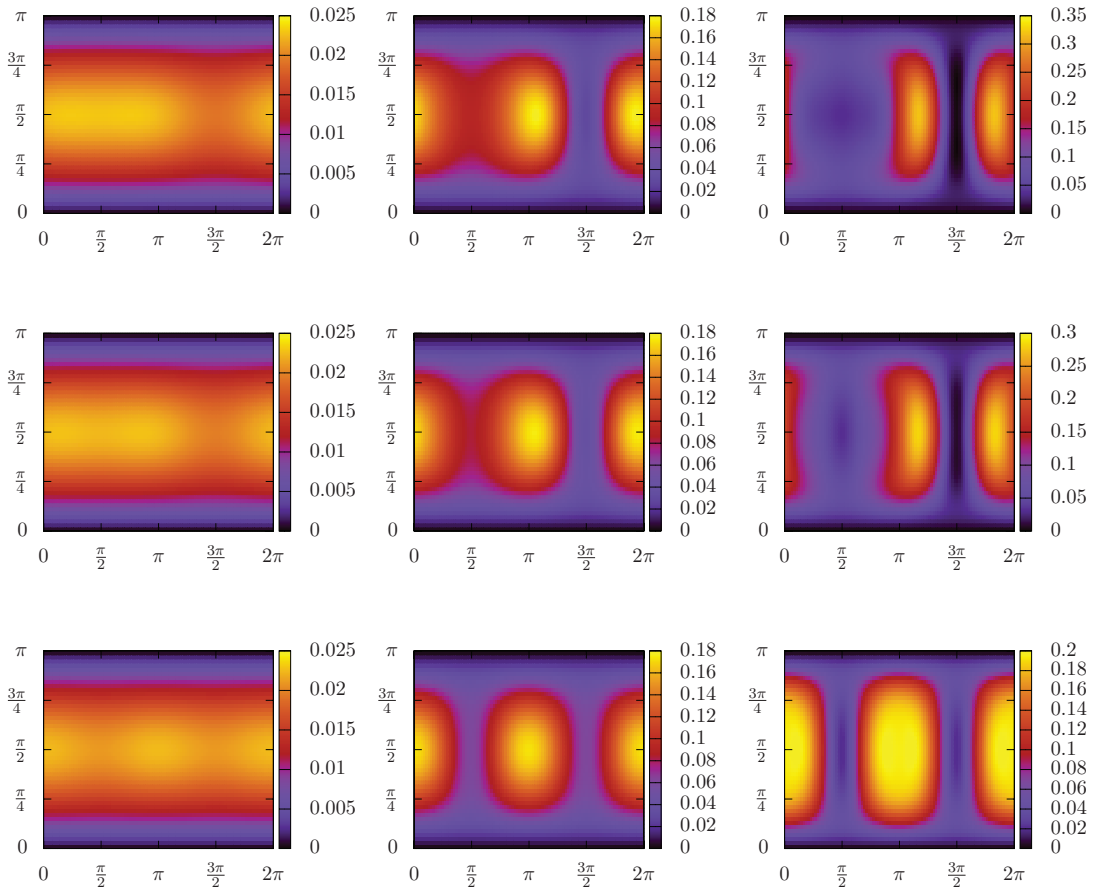

Figure 1. Differential rates $\frac{d\mathcal{R}}{d\phi d\theta}$ for $\frac{\beta}{\beta_2} = 0.1, 0.5$ and 0.9, corresponding to a center-of-mass energy of $E_{cm} = 2.01m, 2.14m$ and $2.59m$ (left to right), and $\delta_1 = 0, \frac{\pi}{8}$ and $\frac{\pi}{4}$ (top to bottom).

3.2. Case II

In the second case, we strongly reduce the frequencies of the lasers with respect to the first case, such that four photons from the first mode or two photons from the second mode are required, leading to $N = 4$ while keeping $\nu = 2$. The increase in N allows for more terms to contribute. In addition to the ordinary processes $(4, 4; 0, 0)$ and $(0, 0; 2, 2)$, we have a mixed term $(2, 2; 1, 1)$, which does not depend on the phase shifts. Furthermore, we have three interference terms with photon numbers $(4, 2; 0, 1)$, $(2, 0; 1, 2)$ and $(4, 0; 0, 2)$. As Fig. 2 shows, the angular distributions of the total process generally exhibit the same properties as in the first case, but they possess a richer structure. The interference contributions have a strong impact, allowing for example for $\beta = 0.5\beta_4$ to force the positrons to be emitted predominantly either in parallel or anti-parallel to the polarization vector of the second laser.

3.3. Total Rates

Now we investigate the total particle count rates. For case I (which is not presented here), we have found a dependence on the frequency, but not on the phase shift. This is caused by the fact that the interference term vanishes after integration over the azimuthal angle.

The second case is examined in Fig. 3. The first panel shows that the ordinary processes

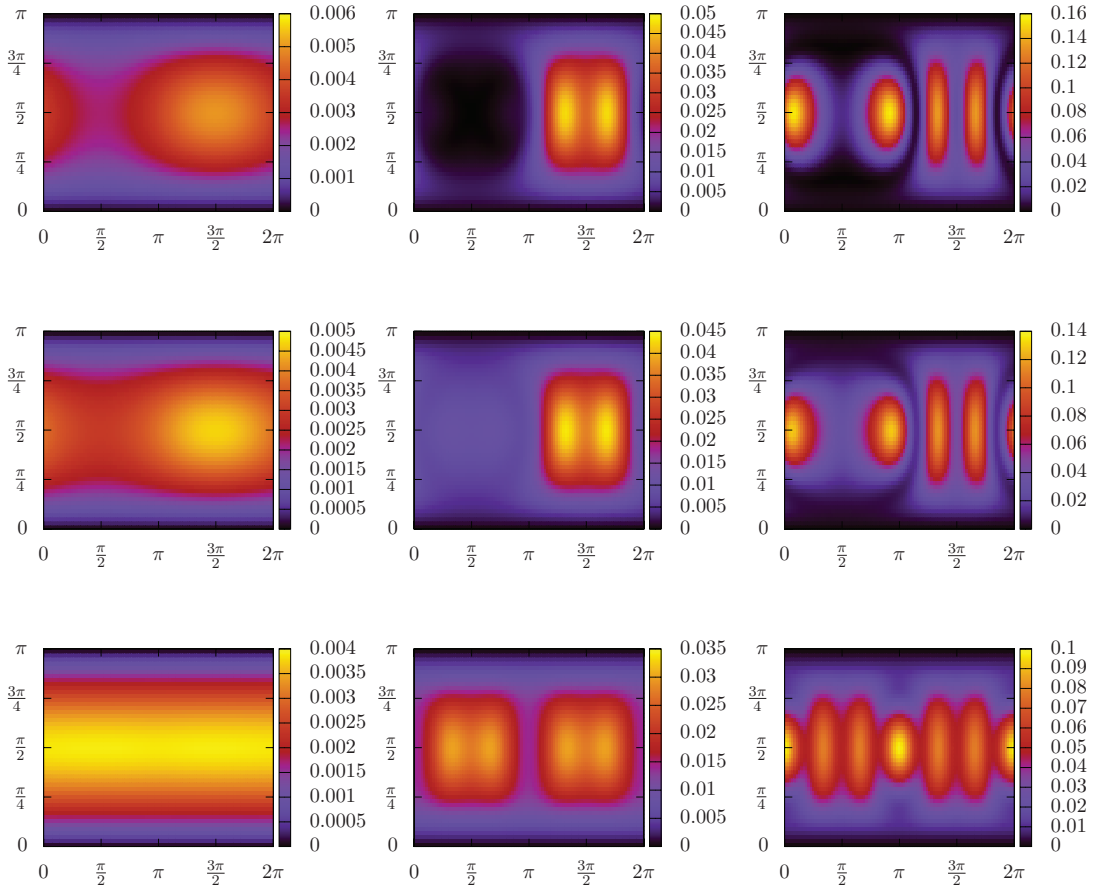

Figure 2. Differential rates $\frac{d\mathcal{R}}{d\phi d\theta}$ for $\frac{\beta}{\beta_4} = 0.1, 0.5$ and 0.9, corresponding to $E_{cm} = 2.003m, 2.07m$ and $2.24m$ (left to right), and $\delta_1 = 0, \frac{\pi}{8}$ and $\frac{\pi}{4}$ (top to bottom).

are dominated by the mixed contribution, which does not depend on the phase shift. When we consider the interference contributions, only the term with photon numbers $(4, 0; 0, 2)$ does not vanish after ϕ-integration, and finally contributes to the total rate. The central panel shows its dependence on the frequencies and on the phase shift, where the latter is given by the phase factor $\cos(4\delta_1)$. Finally the third panel shows the total rate as a function of the frequencies and for various phase shifts, which can be seen to have a significant influence.

To conclude this section, we note that by inspection of the Taylor series of the generalized Bessel functions, a necessary condition for non-vanishing interference contributions to the total rate can be derived. By noting that

$$\int_0^{2\pi} \cos^k(\phi) \sin^l(\phi) d\phi \neq 0 \tag{23}$$

if and only if both integers k and l are even, we arrive at the conclusion that only terms where both sums $n_j + n'_j$ are even can contribute to the total rate. This criterion was not fulfilled for the interference term in case I, whereas in case II, the term with photon numbers $(4, 0; 0, 2)$ introduced the possibility of manipulating the total particle count rate by changing the phase shift.

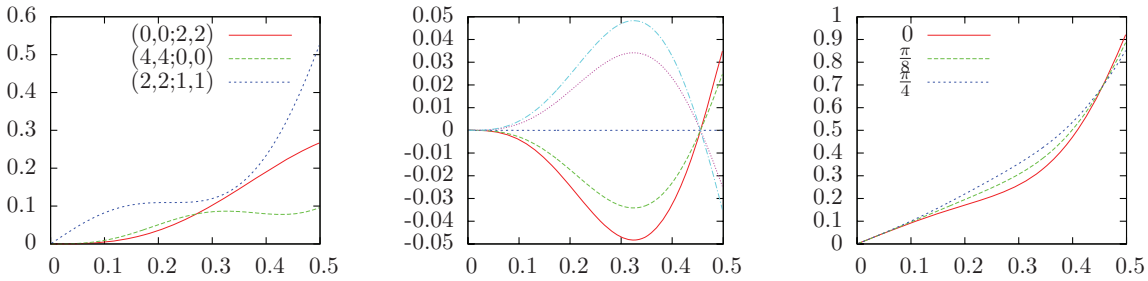

Figure 3. Total rates in units of $\frac{\alpha m}{16\pi}\xi_1^8$ for case II in dependence of β.
Left: Partial contributions. **Center**: Phase-dependence of the interference-contribution $(4,0;0,2)$. The phase shift is increased in steps of $\pi/16$ starting at $\delta_1 = 0$ (red solid curve) up to $\delta_1 = \pi/4$ (cyan dash-dotted curve). **Right**: Total rate for different phase shifts.

4. Dynamical Assistance

The classical Schwinger effect can be regarded as a tunneling transition of an electron from the negative to the positive continuum, transversing a tunneling barrier of height $\sim 2m$ and width $\sim 2m/eE$, where E is the field strength of the (static) electric field. Since even with today's laser technology, the tunneling distance is much bigger than the Compton wavelength, the Schwinger process is exponentially suppressed and escapes experimental observation. In order to lower the tunneling barrier, the scheme of dynamical assistance proposes the addition of high-frequency radiation to the setup [12]. Absorbing these highly energetic photons, the electron is pushed into the energy gap and sees an effectively reduced tunneling barrier.

In the following, we will investigate this scheme by numerically evaluating our expressions for the Breit-Wheeler pair creation process. To begin with, we look at a setup in which one high-intensity optical laser collides with gamma radiation. To avoid numerical problems, we evaluate the expressions in a frame of reference in which the energy of the gamma radiation is heavily reduced to $\omega_\gamma = 0.93869m$, while the frequency of the optical laser is up-shifted to $\omega_2 = 0.07m$. These parameters correspond, for instance, to $\omega_2 = 2.4$ eV and $\omega_\gamma = 7.2$ GeV in the laboratory frame. The red circles in Fig. 4 show the total particle count rate as a function of the inverse of the amplitude ξ_2 of the optical laser. An exponential fit as indicated by the solid line gives a dependence of the form $\mathcal{R} \sim \exp(-16.87/\xi_2)$. The analytic result (2) obtained for Dirac particles was derived under the assumption of $\xi \gg 1$, yet it is known to be approximately valid even for $\xi \approx 1$, and it gives $\mathcal{R} \sim \exp(-20.3/\xi_2)$, which is in rather good agreement with our numerically obtained results. In order to apply the enhancement scheme, we introduce a second laser mode with frequency $\omega_1 = \omega_\gamma$ (which is chosen such that no interferences occur) and amplitude $\xi_1 = 0.004$. In this combined laser field, particles can be created due to the absorption of one photon of frequency ω_1, several photons from the optical laser and the gamma quantum. The corresponding rate is depicted by the blue crosses in Fig. 4. It is enhanced by several orders of magnitude as compared to the case in which only optical photons (and the gamma quantum) have been absorbed[1]. An exponential fit to the data yields $\mathcal{R} \sim \exp(-1.54/\xi_2)$. The total particle rate, as depicted by the open squares in Fig. 4, is mainly given by the channel involving the absorption of one additional high-energy photon.

In order to gain further insight, we investigate the combined process in more detail. The following considerations are still carried out in the frame of reference in which $\omega_\gamma = \omega_1$. Having absorbed the assisting photon and the gamma quantum, the remaining tunneling barrier to be

[1] The data in Fig. 4 is calculated for a setup in which both laser modes are present. The rate labeled by $n_1 = 0$ is essentially the same as for the case when the assisting mode is turned off, $\xi_1 = 0$.

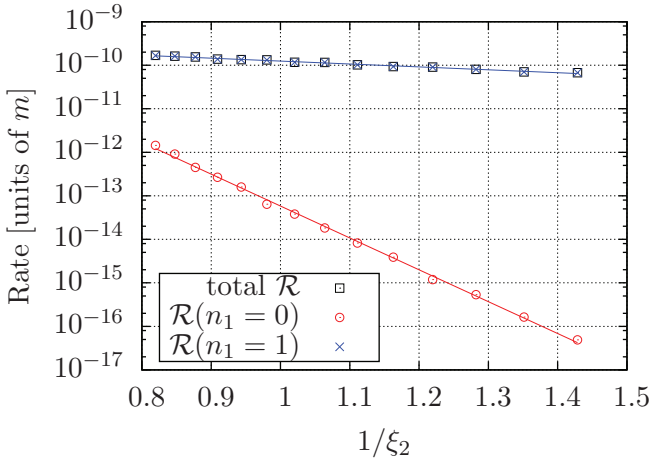

Figure 4. Particle creation rates for $\omega_2 = 0.07m$, $\omega_1 = \omega_\gamma = 0.93869m$, $\xi_1 = 0.004$. The red circles show the contribution from the optical laser (mode 2) alone. The blue crosses depict the rate obtained in the process where one additional photon with frequency ω_1 has been absorbed. The total rate (black squares) is dominated by the channel which is facilitated by the additional radiation. The solid lines are exponential fits to the data.

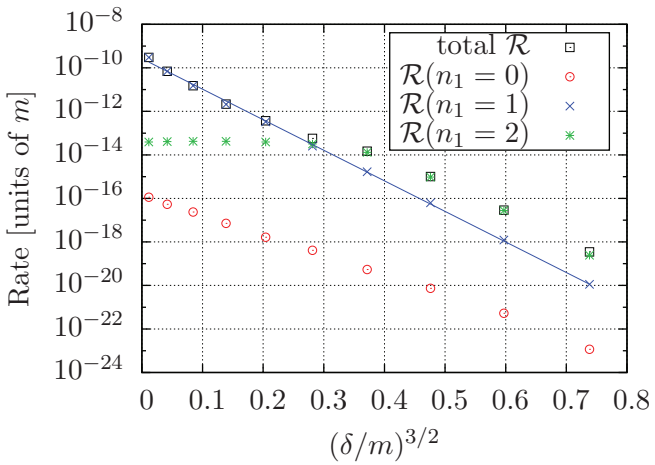

Figure 5. Particle creation rates (black squares) for $\omega_2 = 0.07m$, $\xi_2 = 0.7$, $\xi_1 = 0.004$ and $\omega_1 = \omega_\gamma = \frac{2m-\delta}{2}$ as a function of the gap parameter δ. The red circles, blue crosses and green asteriks show the respective contribution to the rate from the absorption of zero, one or two assisting photons. The solid blue line is an exponential fit.

bridged by the optical laser field is $\delta = 2(m - \omega_1)$. Replacing its slowly oscillating electric field by a constant field $\mathbf{E} = E_0\mathbf{e_2}$, the rate of this process can be obtained by a WKB approximation and yields $\mathcal{R} \sim \exp(-\mathcal{G})$ with the Gamow factor (see also [19])

$$\mathcal{G} = 2\int_0^\ell \sqrt{2m(\delta - eE_0 y)}\, dy = \frac{4\sqrt{2}}{3}\frac{E_{cr}}{E_0}\left(\frac{\delta}{m}\right)^{3/2} \tag{24}$$

where we have used the remaining tunneling distance $\ell = \delta/eE_0$. For our setup, this calculation yields $\mathcal{G} = -1.16/\xi_2$, which is in reasonable agreement with our numerical results. Finally we remark that the pair creation rate induced by the gamma quantum and the assisting laser alone is $4.06 \times 10^{-14}m$.

In order to validate our picture, we have numerically investigated the effect of a change in the tunneling barrier. In Fig. 5 we vary the frequencies of the gamma quantum and the assisting radiation according to $\omega_1 = \omega_\gamma = \frac{2m-\delta}{2}$. The partial rates for the channel comprising one assisting photon can be fitted to a form given by Eq. (24) and we obtain numerically $\mathcal{R} \sim \exp(-32.3\,(\delta/m)^{3/2})$, while the model calculation yields a Gamow factor of $38.5\,(\delta/m)^{3/2}$. The plot clearly shows the enhancement effect, and additionally we see that for bigger values of the gap parameter the channel involving two assisting photons provides the dominating contribution to the total rate.

5. Conclusion

Two different aspects of the Breit-Wheeler pair production process in bichromatic laser fields were investigated. For low-intensity fields with commensurate frequencies, interference effects between production channels involving different numbers of photons have been shown to affect the angular distributions of the emitted particles and in some cases also the total particle count rate. A necessary condition for the latter effect has been derived.

Furthermore, Schwinger-like pair production induced by the decay of a gamma quantum traveling in a high-intensity optical laser wave was studied. Following the scheme of dynamical assistance, the addition of high-frequency yet low-intensity laser radiation was shown to strongly enhance the particle yield, offering good prospects for an experimental realization of Schwinger-like pair production. For more details, the interested reader is referred to [20].

References

[1] Breit G and Wheeler J A 1934 *Phys. Rev.* **46**(12) 1087–1091
[2] Reiss H R 1962 *J. Math. Phys.* **3** 59–67
[3] Nikishov A I and Ritus V I 1964 *Sov. Phys. JETP* **19** 529–541
[4] Narozhny N B, Nikishov A I and Ritus V I 1965 *Sov. Phys. JETP* **20** 622–628
[5] Burke D L, Field R C, Horton-Smith G, Spencer J E, Walz D, Berridge S C, Bugg W M, Shmakov K, Weidemann A W, Bula C, McDonald K T, Prebys E J, Bamber C, Boege S J, Koffas T, Kotseroglou T, Melissinos A C, Meyerhofer D D, Reis D A and Ragg W 1997 *Phys. Rev. Lett.* **79**(9) 1626–1629
[6] Sauter F 1931 *Z. Phys.* **69** 742–764
[7] Schwinger J 1951 *Phys. Rev.* **82**(5) 664–679
[8] Narozhny N B and Fofanov M S 2000 *J. Exp. Theor. Phys.* **90** 415–427
[9] Krajewska K and Kamiński J Z 2012 *Phys. Rev.* A **85**(4) 043404
[10] Augustin S and Müller C 2013 *Phys. Rev.* A **88**(2) 022109
[11] Augustin S and Müller C 2014 *J. Phys. Conf. Ser.* **497** 012020
[12] Schützhold R, Gies H and Dunne G 2008 *Phys. Rev. Lett.* **101**(13) 130404
[13] Villalba-Chávez S and Müller C 2013 *Phys. Lett.* B **718** 992 – 997
[14] Ivanov D Y, Kotkin G L and Serbo V G 2005 *Eur. Phys. J.* C **40** 27–40
[15] Krajewska K and Kamiński J Z 2012 *Phys. Rev. A* **86**(5) 052104
[16] Titov A I, Kämpfer B, Takabe H and Hosaka A 2013 *Phys. Rev. A* **87**(4) 042106
[17] Meuren S, Hatsagortsyan K Z, Keitel C H and Di Piazza A 2014 (*Preprint* `arXiv:1406.7235`)
[18] Reiss H R 1980 *Phys. Rev.* A **22** 1786–1813
[19] Di Piazza A, Lötstedt E, Milstein A I and Keitel C H 2009 *Phys. Rev. Lett.* **103**(17) 170403
[20] Jansen M J A and Müller C 2013 *Phys. Rev.* A **88**(5) 052125